Electric-field-induced transition between the polarization-modulated and ferroelectric smectic-$C_SP_F^*$ liquid crystalline states studied using microbeam x-ray diffraction

Michi Nakata,[1,2,*] Darren R. Link,[1] Yoichi Takanishi,[1] Yumiko Takahasi,[3] Jirakorn Thisayukta,[1] Hiroko Niwano,[1] David A. Coleman,[2] Junji Watanabe,[1] Atsuo Iida,[4] Noel A. Clark,[2] and Hideo Takezoe[1]

[1]*Department of Organic and Polymeric Materials, Tokyo Institute of Technology, O-okayama 2-12-1, Meguro-Ku, Tokyo 152-8552, Japan*

[2]*Department of Physics and FLCMRC, University of Colorado, Boulder, Colorado 80309, USA*

[3]*Department of Physics, College of Science and Technology, Nihon University, 1-8, Surugadai, Kanda, Chiyoda-ku, Tokyo 101-8308, Japan*

[4]*Photon Factory, Institute of Materials Structure Science, Oho 1-1, Tsukuba, Ibaraki 305-0801, Japan*

(Received 26 August 2004; published 31 January 2005)

We report x-ray microbeam studies of a bent-core liquid crystalline material with chiral citronellyl tails. This material has an equilibrium polarization-modulated smectic-*CP* (PM-Sm*CP*) state exhibiting the B_7 texture upon slow cooing from the isotropic while a metastable chiral synclinic ferroelectric Sm-*CP* state (Sm-$C_SP_F^*$) is obtained on quenching from the isotropic. The polarization modulated phase PM-Sm$C_SP_F^*$ shows typical x-ray patterns having multiple satellite peaks around the first-order layer reflection, indicating undulated layers, while the metastable Sm-$C_SP_F^*$ state exhibits a single layering peak indicating flat layers. The Sm-$C_SP_F^*$ state is also induced by the application of an electric field larger than the threshold field (E_{th}) and thermally returns to the polarization modulated PM-Sm$C_SP_F^*$ structure.

DOI: 10.1103/PhysRevE.71.011705 PACS number(s): 61.30.Gd

I. INTRODUCTION

A rich morphology of twisted helical filaments and textured focal conic domains having multiple birefringence colors and stripes parallel to the smectic layers are typical B_7 textures [1]. Smectic liquid crystal phases that have these filaments on slow cooling through the isotropic to smectic phase transition are characterized by unusual powder x-ray patterns that have multiple peaks (usually three peaks or more) in the small-angle region around the smectic layering peak [2]. The multiple peaks in the x-ray scattering indicate that there is additional order beyond a one-dimensional stack of smectic layers. Texture observations in both cells and freely suspended films, in combination with freeze fracture observations, indicated layer undulations as the source of additional order. A stack of synclinic ferroelectric layers as sketched in Fig. 1(a) could, in principle, lower its free energy by organizing in a polarization-splay-modulated state, as sketched in Fig. 1(b) [2]. Such polarization splay modulation is thought to explain the features not only in the B_7 phase but also in some two-dimensional phases like the $B_{1\text{revtilt}}$ phases [3–5]. However, it is unclear what happens to the undulated layers on application of an electric field that is sufficient to drive the system into the uniform ferroelectric state.

From the electrooptic response and polarization reversal current measurements, some materials exhibiting the B_7 texture are thought to be ferroelectric, at least after application of an electric field [6,7]. However, other materials exhibiting this texture are thought to have an antiferroelectric ground state or to exhibit spontaneous polarization components along the layer normal—i.e., the so-called smectic-*C* general phase (Sm-*Cg*)—upon cooling from the isotropic. Indirect evidence for these interpretations is found in the high-threshold field that is necessary to induce a transition to the ferroelectric state and in an electrical response characterized by a polarization with a component along the layer normal [8,9].

To elucidate the structural changes that take place in the layer organization at high-field strengths, $E > E_{\text{th}}$, we performed microbeam x-ray scattering experiments on single domains both in the ground-state configuration and under the application of a field. We report that the scattering peaks associated with the ground-state layer undulations disappear on application of a sufficiently large field, consistent with a

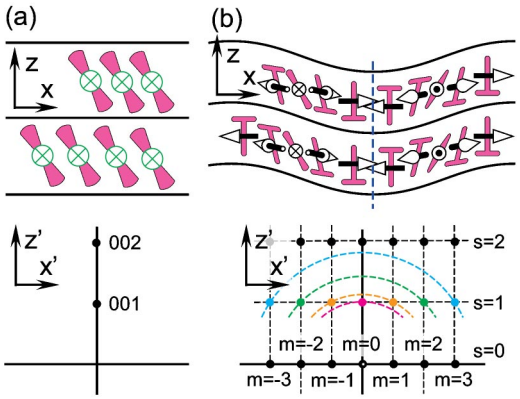

FIG. 1. (Color online) Sketch of the layer structure and scattering pattern of the uniform and polarization-splay-modulated Sm-$C_SP_F^*$ states. The uniform Sm-$C_SP_F^*$ state, sketched in (a), is expected to give rise to a single-layering peak in the x-ray pattern with possibly additional higher harmonics as sketched below the structure. The polarization-modulated structure, sketched in (b), is expected to result in off-axis peaks in the x-ray pattern as sketched below the structure.

*Corresponding author.

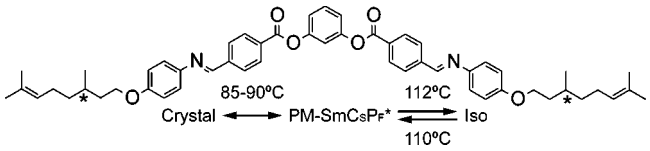

FIG. 2. Chemical structure and transition temperatures of (*R*)-Citronellyl-OPIMB.

field-induced transition to a synclinic ferroelectric state that does not have polarization splay. This state is metastable to nucleation and growth of ground-state domains on removal of the field.

II. EXPERIMENT

We report measurements taken at the temperature T, 10 K below the isotropic-to-smectic transition temperature T_c ($T_c - T = 10$ K) for the chiral bent-core liquid crystal (*R*)-Citronellyl-OPIMB; see Fig. 2. Texture observations were carried out using thin capacitor-type cells with a 4–10-μ gap. For x-ray measurements, we used a free surface droplet as well as capacitor-type cells constructed of thin glass (50–80 μ). The x-ray diffraction experiments were carried out on beamline 4A (BL-4A) at the Photon Factory (PF) a part of the High Energy X-ray Laboratory (KEK) at Tsukuba (Japan). The incident x-ray beam size was roughly 3×4 μ^2 at the sample and the angular divergence is about 1.0 mrad in both horizontal and vertical directions. The x-ray energy was 8 keV ($\sim$1.55 Å), and we used a two-dimensional area detector [charge-coupled device] (CCD), Hamamatsu Photonics, C4880-50] to obtain two-dimensional diffraction patterns. On the area detector, the distance between the beam center and diffraction spots indicates the scattering angle (2θ), and the x-ray scattering intensity profile around a circle centered at the beam center provides information about the smectic layer orientation in the plane of the cell (χ profile). The sample cell can be rotated around an axis parallel to the plane of the cell and perpendicular to the x-ray beam (ω profile). The x-ray scattering intensity of the ω profile indicates the smectic layer orientation within the cell.

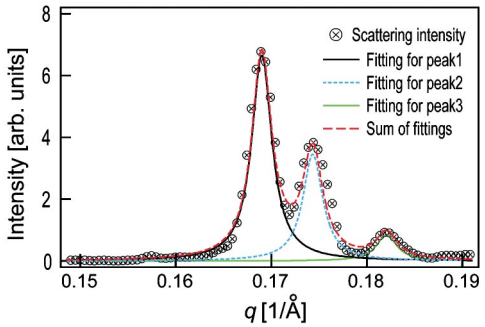

FIG. 3. (Color online) Powder x-ray scattering from a free surface drop in the PM-Sm-$C_SP_F^*$ phase. Each scattering peak is fit using a Lorentz function to obtain the scattering angle. The small dip at $q = 0.158$ A^{-1} is an artifact from the stop for the direct beam.

TABLE I. X-ray scattering angle and index corresponding to peaks in Fig. 3.

	Index	2θ [deg]	q [Å^{-1}]	Distance in real space [Å]
Peak 1	$s=1$, $m=1$	2.39	0.169	37.2
Peak 2	$s=1$, $m=2$	2.46	0.174	36.1
Peak 3	$s=1$, $m=3$	2.57	0.182	34.5

III. RESULTS AND DISCUSSION

A. X-ray diffraction from the bulk sample

In order to measure the powder x-ray scattering intensity as a function of scattering angle in the ground state of the smectic phase of (*R*)-Citronellyl-OPIMB we measured scattering from the free surface drop. As shown in Fig. 3, we observe at least three distinct diffraction peaks in the small-angle region which are summarized in Table I, suggesting a two-dimensional ordering within the smectic layers in the phase, similar to what has been proposed for other materials having the B_7 texture [2] [see Fig. 1(b)]. Peak 1 at $q = 0.169$ A^{-1} ($2\theta = 2.39°$) is assigned to the $s=1$, $m=\pm 1$ Bragg reflection [see Fig. 1(b)] which overlaps with the $m=0$ peak. The $m=0$ peak in this case shows lower scattering intensity comparing to the $m=\pm 1$, which is actually related to the undulation amplitude [2,5]. The other two peaks in the ground-state PM-Sm-$C_SP_F^*$ structure, peaks **2** and **3**, are assigned to be $m=\pm 2$ and ± 3 [see Fig. 1(b)], respectively. A significant difference between our material and what was previously studied is that our material is chiral, and hence we expect that the layer chirality is uniform throughout all of the

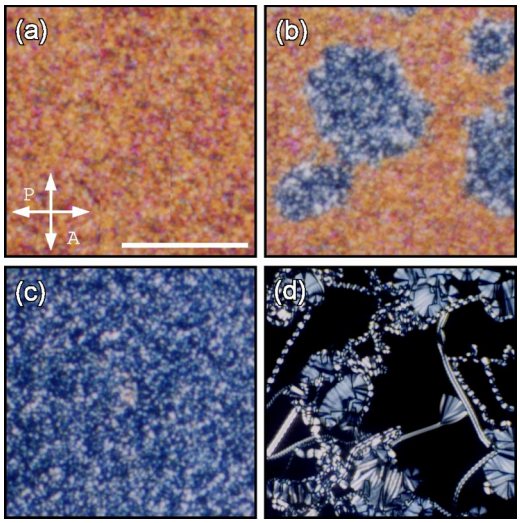

FIG. 4. (Color online) Photomicrographs of the metastable Sm-$C_SP_F^*$ and the ground-state PM-Sm-$C_SP_F^*$ domains in the smectic phase of (*R*)-Citronellyl-OPIMB in a 6-μ-thick cell. (a) Grainy high-birefringent domains of metastable state obtained by fast cooling from the isotropic. (b) The ground-state domain nucleates and totally filled the cell (c). The B_7 texture is obtained by slow cooling from the isotropic. White bar in the photo indicates the real length of 100 μm.

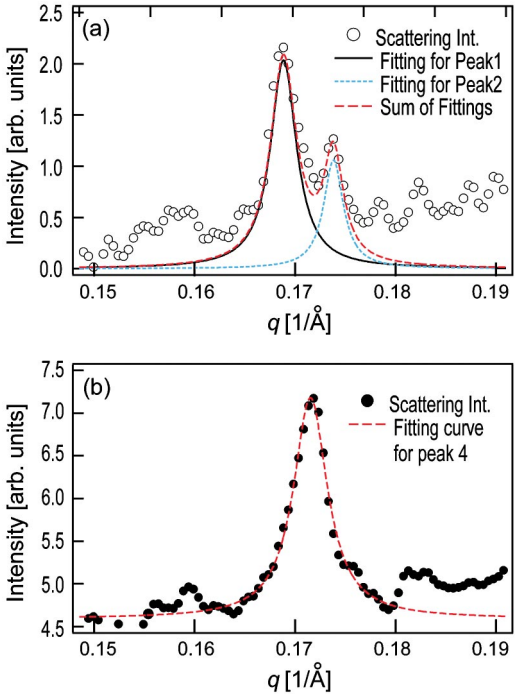

FIG. 5. (Color online) Powder x-ray scattering intensity as a function of scattering angle measured in (a) the ground-state PM -Sm-$C_SP_F^*$ and (b) metastable Sm-$C_SP_F^*$ state in the smectic phase of (*R*)-Citronellyl-OPIMB in a 10-μ-thick cell. Each scattering peak was fit to a Lorentz function to obtain the scattering angle.

layers even in the polarization modulated phase. We confirmed this uniform chirality with electrooptic experiment which shows unichiral responses that all domains have the same sign of layer chirality [10].

B. X-ray diffraction from LC cells

Upon quenching the material from the isotropic in capacitor-type cells, grainy domains of the metastable Sm -$C_SP_F^*$ state with high birefringence are observed to nucleate from the isotropic [see Fig. 4(a)]. We previously confirmed that the metastable state is ferroelectric by means of optical second-harmonic generation measurement [10]. The ground-state PM-Sm-$C_SP_F^*$ structure has lower birefringence and typical B_7 textures forms on annealing [see Fig. 4(b)–4(d)].

In order to obtain x-ray diffraction profiles from the metastable state and the ground state separately, we used a microbeam x-ray to select a specific domain in the cell [Fig. 4(b)]. In both cases we find the scattering pattern to be independent of χ and ω and we interpret this to mean that the layers in the scattering volume do not have a preferred orientation. There is a marked difference in the x-ray microbeam scattering pattern of the two states, Sm-$C_SP_F^*$ and PM-Sm-$C_SP_F^*$, as a function of scattering angle. As expected, we find that the metastable state has only one peak [Fig. 5(b)] and corresponds to the reflection of flat smectic layers [see Fig. 1(a)]. After allowing the ground-state structure to nucleate and fill the cell we find multiple peaks as in the bulk [Fig. 5(a) and summary of peaks in Table II]. The single peak in the metastable state occurs at a scattering angle that is different from any of the multiple PM-Sm-$C_SP_F^*$ peaks. The positions of the two peaks in Fig. 5(a) correspond exactly to the first two peaks observed in the bulk droplet—i.e., the $s=1$, $m=\pm1$ and $s=1$, $m=\pm2$ Bragg reflections. Also, as shown in Fig. 5(a) and Table II, the $s=1$, $m=\pm1$ peak at $q=0.169$ Å^{-1} has the highest scattering intensity. This suggests that this peak characterizes the largest volume fraction in the undulated structure. The smectic layer thickness in the metastable flattened Sm-$C_SP_F^*$ state is determined to be 36.5 Å. The ground state is a typical B_7 phase with undulated smectic layers.

TABLE II. X-ray scattering angle and index corresponding to peaks in Fig. 5.

		Index	2θ [deg]	q [Å^{-1}]	Distance in real space [Å]
Ground state	Peak 1	$s=1$, $m=1$	2.39	0.169	37.2
	Peak 2	$s=1$, $m=2$	2.46	0.174	36.1
Metastable state	Peak 4	(001)	2.43	0.172	36.5

For a detailed analysis of the structure, it is critical to have an alignment of the layer normal over regions significantly larger than the microbeam. We obtained single-domain regions with uniform alignment over the area of the microbeam by applying an electric field on cooling [Fig. 6(a)]. Shown in Fig. 7 is an area detector image of x-ray scattering intensity from a focal conic domain of the ground state after application of a square-wave voltage ($E \sim 25$ V/μ) in a 6-μ-thick cell under microbeam illumination. On the image shown in Fig. 7(a), at least seven diffraction spots are distinguishable, corresponding to $s=1$, $m=0$, ±1, ±2 and ±3. The scattering intensity of these diffraction spots is shown in Fig. 7(c) which agrees well with the expected reflection pattern from such an undulated-smectic layer structure [2] but had not been observed directly in oriented samples. The scattering intensity profile as a function of the scattering angle (integrated over χ) is shown in Fig. 7(d) and summarized in Table III. The wave vector of the $m=0$ spot is estimated to be $q=0.168$ Å^{-1} ($2\theta=2.37°$), very close to the magnitude of the $m=\pm1$ reflections, and hence these diffraction peaks overlap in the powdered samples. The

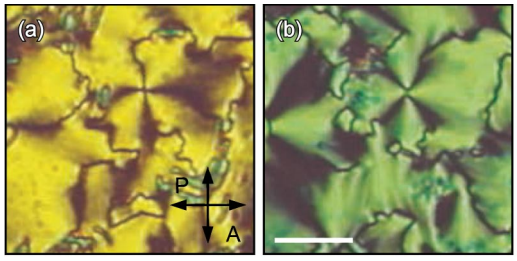

FIG. 6. (Color online) Photomicrographs of focal conic circular domains of (a) the ground state and (b) field-induced metastable Sm-$C_SP_F^*$ state in the smectic phase of (*R*)-Citronellyl-OPIMB in a 6-μ-thick cell, obtained by application of an electric field. White bar in the photo indicates the real length of 150 μm.

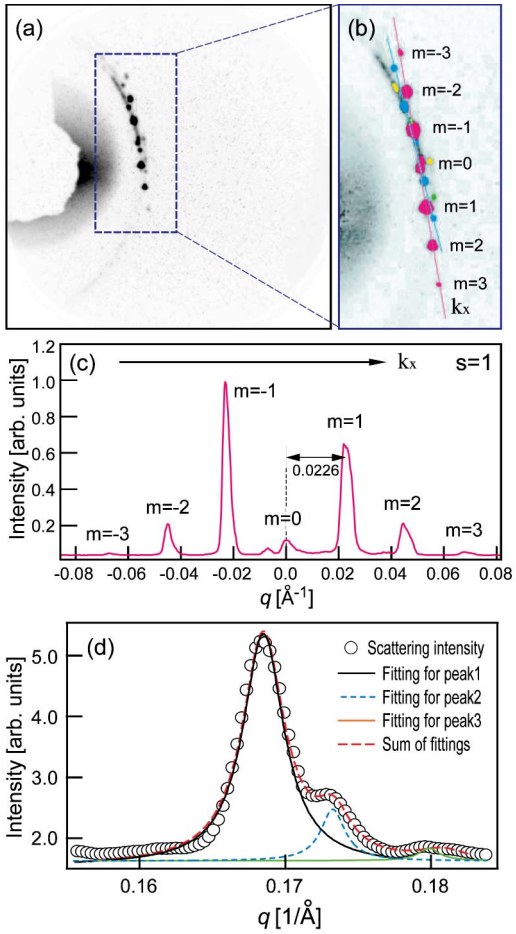

FIG. 7. (Color online) Detailed two-dimensional x-ray diffraction pattern of the ground-state PM-Sm-$C_S P_F^*$. Several sets of diffraction spots from different domains were obtained as shown in (b). The majority of those domains in the illuminated area produced scattering intensity profile along line k_x in (b) which is perpendicular to the z axis (layer normal direction) as shown in (c). Diffraction intensity as a function of angle is shown in (d) obtained by integrating the two-dimensional diffraction profile around the beam center.

undulation wavelength is estimated from the distance between neighboring diffraction spots in reciprocal space. As shown in Fig. 7(c), the spacing is measured to be around $q = 0.0226$ Å^{-1} so that the modulation wavelength is around 280 Å. The ω profile (not shown) indicates that that the layer normal is approximately parallel to the plane of the cell with a distribution of $\sim 10°$.

Under an electric field larger than E_{th} (~ 37 V/μ), domains with high birefringence ($\Delta n \sim 0.20$) and tilted extinction directions ($\sim 45°$) were observed to be stable [Fig. 6(b)]. This field-induced state was found to have the chiral synclinic ferroelectric (Sm-$C_S P_F^*$) ordering according to these optical observations in agreement with second-harmonic generation measurements [10]. The field-induced state, however, is metastable and slowly relaxes back to the ground state. This relaxation process takes around 30 min at $T_c - T \sim 10$ K. Shown in Fig. 8 are area detector images of the x-ray scattering intensity from a focal conic domain in a 4-μ thick cell under microbeam illumination. In the field-induced ferroelectric state, a single-scattering peak was observed with a broad distribution. According to the χ profile shown in Fig. 8(c), the layer normal direction in the illuminated area has a distribution width of around 10°. Also, according to the ω profile (not shown) the smectic layers stand

TABLE III. X-ray scattering angle and index corresponding to peaks in Fig. 7.

	Index	2θ [deg]	q [Å^{-1}]	Distance in real space [Å]
Peak 1	$s=1$, $m=1$	2.38	0.168	37.3
Peak 2	$s=1$, $m=2$	2.46	0.174	36.1
Peak 3	$s=1$, $m=3$	2.57	0.182	34.6

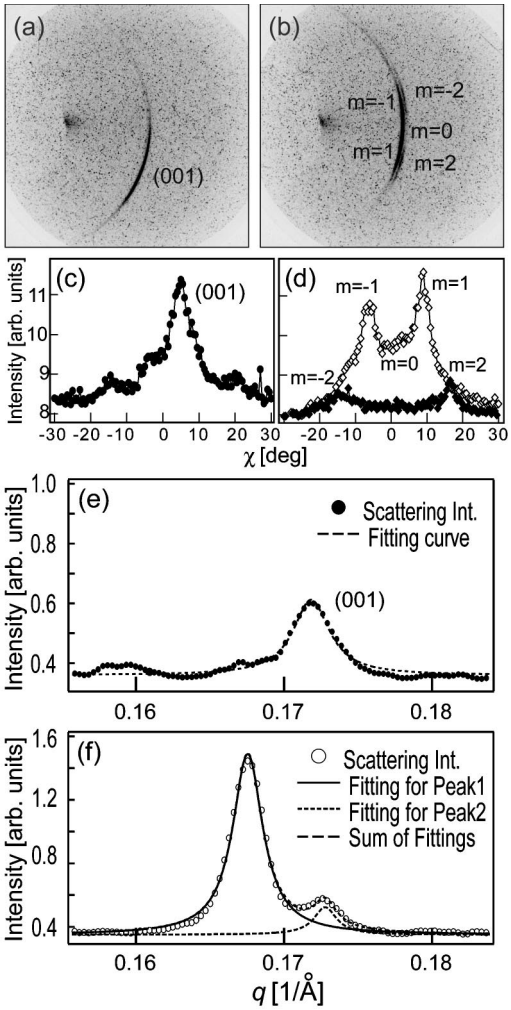

FIG. 8. Two-dimensional oriented x-ray scattering patterns of (a) the field-induced metastable Sm-$C_S P_F^*$ state and (b) the ground state obtained using microbeam x-ray illumination onto one domain in a 6-μ-thick cell. Shown in (c) and (d) are the scattering intensity profiles on χ for (a) and (b), respectively. The scattering intensity labeled with open diamonds is about inner scattering, and solid diamonds indicate the scattering intensity of the outer diffraction. (e) and (f) show the scattering intensity profile obtained from (a) and (b), respectively, as a function of scattering angle.

TABLE IV. X-ray scattering angle and index corresponding to peaks in Fig. 8.

		Index	2θ [deg]	q [Å^{-1}]	Distance in real space [Å]
Ground state	Peak 1	$s=1$, $m=1$	2.37	0.168	37.5
	Peak 2	$s=1$, $m=2$	2.44	0.173	36.4
Metastable state	Peak 4	(001)	2.43	0.172	36.5

up almost normal to the substrate; this is the so called "bookshelf" structure with the disorder in the ω profile reduced from 15° to 10°. This decrease in the width of the ω profile and corresponding increase in the width of the χ profile is characteristic of field-induced straightening of the smectic layers such as in the transition from a vertical chevron to a horizontal chevron [11,12]. There is no hint of Sm-*Cg*-type layer orientation where the smectic layers must be tilted from the field direction under application of a large electric field because the spontaneous polarization includes a component out of the layer plane [9]. After relaxation to the ground state from the field-induced metastable Sm-$C_SP_F^*$ state, the original reciprocal lattice of the PM-Sm-$C_SP_F^*$ state is recovered, as shown in Fig. 8(b). As with the field-induced Sm-$C_SP_F^*$ state, the peaks retain a broad distribution in χ and a narrow distribution in ω, indicating that the bookshelf alignment is retained. Figures 8(e) and 8(f) show the scattering intensity profile obtained from Figs. 8(a) and 8(b), respectively. The scattering angle of each diffraction spot is summarized in Table IV, which corresponds to scattering peaks observed in the powder pattern in Table II. The $m=0$ reflection is not clearly observable because the scattering intensity is small for $m=0$ (see Fig. 7) and the increased in-plane disorder (χ) overlaps the $m=0$ with the $m=\pm1$ reflections.

C. Discussion

According to these observations, the metastable state obtained from quenching from the isotropic and field-induced states has the same layer structure, Sm-$C_SP_F^*$, synclinic in tilt and ferroelectric in polar order in smectic layers without undulation [Fig. 1(a)]. The layer thickness is estimated to be 36.5 Å, and the tilt angle of the molecules is estimated from the extended molecular length (49 Å) to be 42° which is slightly smaller but close to the optical tilt angle (45°).

The ground-state PM-Sm-$C_SP_F^*$ exhibits peaks corresponding to the zeroth order ($s=1$, $m=0$) which overlapped with the first order ($s=1$, $m=\pm1$) and higher orders ($s=1$, $m=\pm1, \pm2, \ldots,$) in the powder pattern shown in Tables I and II, as well as in focal conic textures in cells either without electric field or after relaxation from the field-induced state. The periodicity of undulation is estimated to be around 280 Å. Unfortunately, we could not observe $s=0$ peaks because of the limited resolution of our experiment system.

Based on the polarization modulation model [2], the undulated layer structure associated with the B_7 texture is produced by polarization splay in the plane of smectic layers. In this interpretation, there is a free energy cost associated with defect lines at the interface of two splay areas that must be compensated for by a reduction in the free energy through the formation of polarization splay. Under application of an electric field, however, the spontaneous polarization reorients uniformly along the field. As the polarization splay domains are removed by the field, translational invariance within the layers is restored and the smectic layer undulations flatten, removing the intralayer ordering. Our result that the field-induced ferroelectric Sm-$C_SP_F^*$ state lacks undulation of the smectic layers is in complete agreement with this prediction. In addition, we find that there is no evidence for Sm-*Cg* ordering; neither a bilayer diffraction peak nor tilted smectic layer under application of an electric field is observed in the field-induced Sm-$C_SP_F^*$ state or the ground state PM-Sm -$C_SP_F^*$ structure.

IV. CONCLUSION

The smectic phase of (*R*)-Citronelly-OPIMB was examined by means of texture observations and x-ray diffraction measurements. This phase exhibits a chiral metastable Sm -$C_SP_F^*$ state that relaxes to a stable PM-Sm-$C_SP_F^*$ ground state that has a polarization modulation and layer undulations associated with the B_7 texture. The metastable Sm-$C_SP_F^*$ state is also induced from the ground-state structure by application of an electric field greater than a threshold field E_{th}; the ground state nucleates and grows with an undulated layer structure of wavelength around 280 Å on removal of the field. Such a field-induced transition to a nonundulated Sm-*CP* state might be observed not only in the B_7-type phases but also in the other variation phases with polarization modulation such as the $B_{1\mathrm{rev}}$ and/or $B_{1\mathrm{revtilt}}$ phases.

ACKNOWLEDGMENTS

The authors are thankful to Professor D. M. Walba for useful discussions. M.N. and D.L. acknowledge the support of the Japanese Society for the Promotion of Science (JSPS). This work was partly supported by a Grant-in-Aid for Scientific Research on Priority Area (B) (No. 12129202) by the Ministry of Education, Science, Sports and Culture of Japan. M.N., D.A.C., and N.A.C. acknowledge the support of the NSF under Grant Nos. DMR-0213918 and DMR-0072989. This work was carried out under the approval of the PF Advisory Committee (Proposal Nos. 00G088 and 02G135).

[1] G. Pelzl, S. Diele, A. Jakli, C. Lischka, I. Wirth, and W. Weissflog, Liq. Cryst. **26**, 135 (1999).
[2] D. A. Coleman, J. Fernsler, N. Chattham, M. Nakata, Y. Takanishi, D. R. Link, R.-F. Shao, W. G. Jang, J. E. Maclennan, E. Körblova, O. Mondain, C. Boyer, W. Weissflog, G. Pelzl, L.-C. Chien, D. M. Walba, J. Zasadzinski, J. Watanabe, H. Takezoe, and N. A. Clark, Science **301**, 1204 (2003).
[3] K. Pelz, W. Weissflog, U. Baumeister, and S. Diele, Liq. Cryst. **30**, 1151 (2003).
[4] J. Szydlowska, J. Mieczkowski, J. Matraszek, D. W. Bruce, E. Gorecka, D. Pociecha, and D. Guillon, Phys. Rev. E **67**, 031702 (2003).
[5] D. A. Coleman, C. Jones, J. Fernsler, D. R. Link, E. Körblova, D. M. Walba, N. A. Clark, M. Nakata, Y. Takanishi, H. Takezoe, W. Weissflog, G. Pelzl, and L.-C. Chien (unpublished).
[6] D. M. Walba, E. Körblova, R. Shao, J. E. Maclennan, D. R. Link, M. A. Glaser, and N. A. Clark, Science **288**, 2181 (2000).
[7] C. K. Lee, A. Primak, A. Jakli, E. J. Choi, W. C. Zin, and L. C. Chen, Liq. Cryst. **28**, 1293 (2001).
[8] A. Jakli, D. Kruerke, H. Sawade, and G. Heppke, Phys. Rev. Lett. **86**, 5715 (2001).
[9] A. Jakli, G. G. Nair, H. Sawade, and G. Heppke, Liq. Cryst. **30**, 265 (2003).
[10] D. R. Link, M. Nakata, Y. Takanishi, J. Watanabe, and H. Takezoe (unpublished).
[11] P. C. Willis, N. A. Clark, and C. R. Safinya, Liq. Cryst. **11**, 581 (1992).
[12] Y. Takahashi, A. Iida, Y. Takanishi, T. Ogasawara, M. Nakata, K. Ishikawa, and H. Takezoe, Phys. Rev. E **67**, 015706 (2003).